*Mon. Not. R. astr. Soc.* (1992) **258**, 159–166

# Monte Carlo solutions for the radiative processes in 1612-MHz OH masers

Marco Spaans and Huib Jan van Langevelde
*Sterrewacht Leiden, PO Box 9513, 2300 RA Leiden, The Netherlands*

Accepted 1992 March 4. Received 1992 February 5; in original form 1991 December 10

**SUMMARY**

We use a Monte Carlo method to solve the radiative transport in circumstellar OH masers. In this way we model the observed double-peaked 1612-MHz maser emission from expanding molecular shells around highly evolved stars. Earlier attempts to describe in detail the *shape* of the spectra have had limited success, because of the complexity of the radiative transfer problem, in that the radiation of the maser couples to the population inversion which – together with the global geometry of the model – determines the radiation field. It turns out that our approach deals with this automatically, with the big advantage that the whole problem is coded in terms of local physics. We show that our code can reproduce features like maser saturation and beam crossing, and we discuss its limits. With plausible parameter values from the literature we readily obtain spectra that resemble the observed spectra quite well. Thus we conclude that the average shape of OH/IR star spectra can be fully explained by a model of a spherically symmetric, homogeneous and constantly expanding shell.

**Key words:** line: profiles – masers – radiative transfer – methods: statistical – circumstellar matter – radio lines: molecular: circumstellar.

## 1 INTRODUCTION

### 1.1 Circumstellar 1612-MHz masers

In 1968 the first OH 1612-MHz double-peaked spectrum, characteristic of OH/IR stars, was observed (Wilson & Barrett 1968). Already then it was suggested that the shape of the spectrum was caused by outflowing material around a star. Several observations have shown that this is indeed the case, but no fully consistent description of the exact shape of the spectrum has yet been given (see Cohen 1989 for a review).

OH/IR stars, especially the strong, regular type II masers, are an interesting class of objects. They are obviously maser sources (the brightness temperatures leave no doubt) but, on the other hand, they are relatively smooth in their variability, spectral shape, and brightness distribution. Indeed it is remarkable how regular these sources appear, considering that we are looking at a radiative process of exponential growth. Among all cosmological masers the circumstellar 1612-MHz masers in OH/IR stars are certainly the most regular.

This regularity is due to saturation. The maser process is self-regulating in these objects so that a well-behaved radiation pattern emerges. This makes the OH/IR stars fascinating objects to study. Observationally it opens the possibility of measuring some subtle effects, such as distances from phase lags. Theoretically it results in an intriguing radiative transfer problem.

### 1.2 Observations of OH/IR stars

Fig. 1 shows a typical OH/IR 1612-MHz spectrum, for later comparison with the model spectrum (OH 359.954 − 0.041 is taken from the Galactic Centre sample by Lindqvist *et al.* 1991, and was observed with the VLA, see van Langevelde *et al.*, in preparation). A typical spectrum for these sources is hard to define, because most show asymmetries and extra emission features. A range of underlying shapes is present in the observed spectra: different ratios of the flux in the inner parts of the spectra to the peaks are observed, as well as different widths of the peaks. Furthermore, the maser luminosities apparently range over at least two decades (see for instance the luminosity function in Lindqvist, Winnberg & Habing 1989). An average spectrum for a sample of OH/IR stars was published by Johansson *et al.* (1977), but their sensitivity and resolution are insufficient for our purposes. On average the OH spectrum reveals two equally strong peaks separated by 20–50 km $s^{-1}$ with a steep decline on the outer edges and a more tapered decline towards the inner

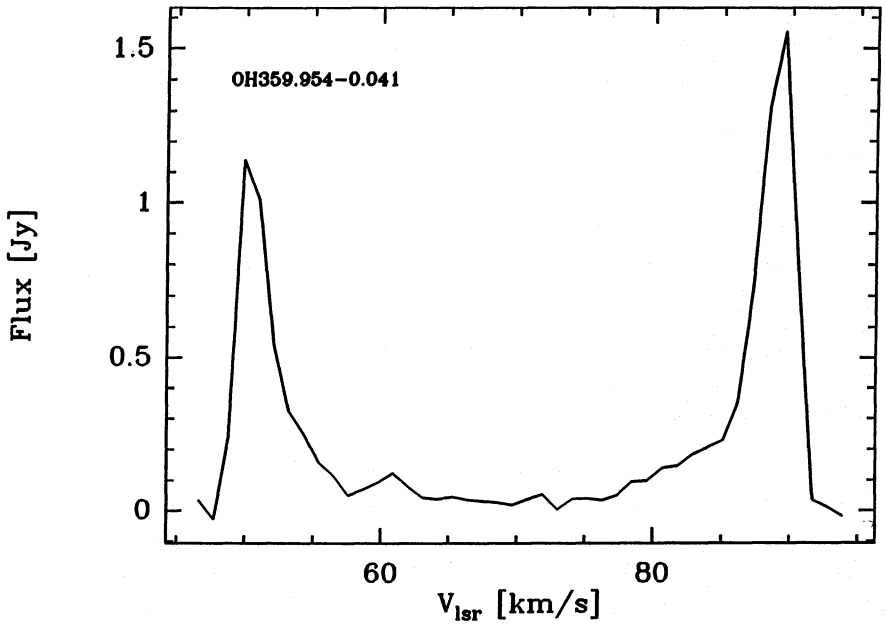


**Figure 1.** The spectrum of OH 359.954 − 0.041, a 'typical' example of a 1612-MHz OH/IR star spectrum.

part of the spectrum. The inner parts of the spectrum are at a level of a few per cent of the peak flux.

The double-peaked 1612-MHz spectra originate in the circumstellar shells around evolved stars. This can be concluded from the distribution of these objects on the sky; furthermore, comparable profiles are detected in the direction of Miras – evolved variable stars. Some of the stars that exhibit maser action cannot be optically detected; apparently the dust (also seen in the Miras) obscures the star. All these objects turn out to be luminous IR sources.

Thus the picture emerges of an evolved star which loses mass, resulting in a shell of dust and gas, flowing continuously from the star. Inflow or rotation can be ruled out as a cause of the double-peaked spectrum. The confirmation of this is the measurement of phase lags (Schultz, Sherwood & Winnberg 1978; Jewell, Webber & Snyder 1980; Herman & Habing 1985; van Langevelde, van der Heiden & van Schooneveld 1990). The phase lag is the time delay between the periodic variations of the blue- and redshifted peaks in the spectrum, which can be measured when the variability of the sources is monitored accurately. Brightness changes of the blueshifted peak precede those in the red, so that the blueshifted gas must be closer to us than the redshifted.

The double-peaked spectrum originates from the expanding circumstellar shell as follows: for radiation in the direction of the observer the longest coherent path-length in the outflowing OH is found in the extreme front and back of the shell. This results in peak emission at velocities $-v_e$ and $+v_e$ in the spectrum (see Fig. 2).

Another important result from monitoring studies is that the variations of the OH maser and the infrared emission from the circumstellar shell occur in phase and that they are of comparable relative amplitude. This implies first that the maser is pumped by the infrared emission and secondly that it is saturated. We shall come back to these points in more detail later.

In several stars the shells can be mapped by interferometric observations (Booth *et al.* 1981; Bowers, Johnston & Spencer 1983; Herman *et al.* 1985; Diamond *et al.* 1985; Bowers & Johnston 1990). Combined with a measurement of the phase lag, such a map yields the distance to the star with a minimum of assumptions needed. The motivation for the research described here was to look into possible biases

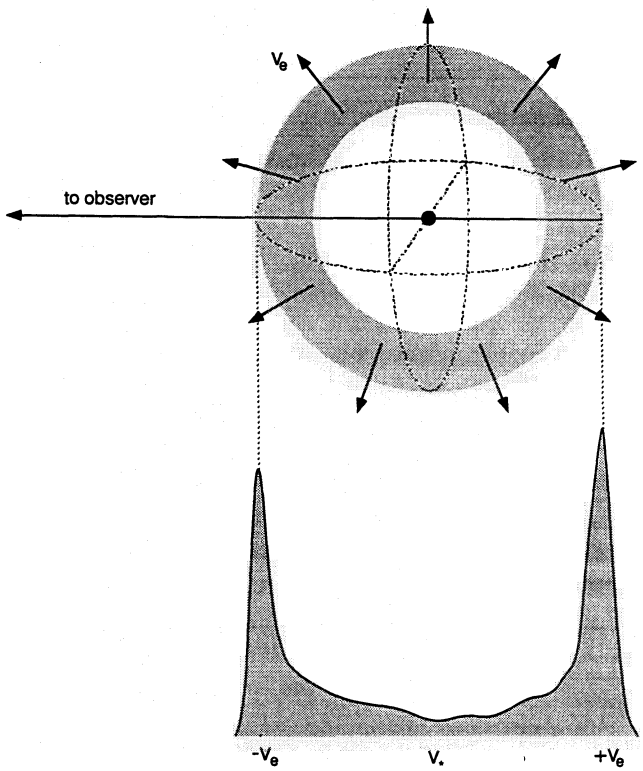


**Figure 2.** Schematic view of the origin of the maser spectrum.

in the phase-lag distances, possibly caused by the non-isotropic nature of the radiation (van Langevelde *et al.* 1990). The full discussion of these features will be presented in a later paper (van Langevelde & Spaans, in preparation). Here we concentrate on setting up a model for the 1612-MHz maser.

### 1.3 Outline

In Section 2 we consider the problem of radiative transfer and discuss its mathematical form; we point out the effects of saturation and beam crossing and explain why we cannot use a one-dimensional radiative transfer solution. We propose in Section 3 a Monte Carlo scheme that deals with the complex two-dimensional radiative transfer problem. This is first applied in a slab with changing axis ratio (Section 4), showing that is produces the saturation and beam crossing features which a maser should exhibit.

To set up the model for a real spherically symmetric shell, we have to consider the physical input parameters. Here we do not discuss a large range of parameters, but concentrate on a model with justifiable input values. In Section 5 we show that, without any further tuning, our model produces a reasonable OH spectrum. We end with a discussion on the validity of the 'standard' model for OH/IR stars, and draw the conclusion that there is no need for any revisions.

In a subsequent paper we shall concentrate on the physical and geometrical properties of circumstellar OH masers, test the dependencies of the model on the input parameters, and discuss some aspects of phase lags.

## 2 DESCRIPTION OF THE PROBLEM

### 2.1 The formal problem

Consider the problem of radiative transfer in an inverted medium (Elitzur 1982). The transport equation for radiative transfer is

$$\frac{dI_\nu}{ds} = -\alpha_\nu(\boldsymbol{x})I_\nu + \sigma_\nu(\boldsymbol{x}), \tag{1}$$

where the absorption coefficient is given by

$$\alpha_\nu(\boldsymbol{x}) = \frac{h\nu}{4\pi} n_1(\boldsymbol{x}) B_{12} \left[1 - \frac{g_1 n_2(\boldsymbol{x})}{g_2 n_1(\boldsymbol{x})}\right] \Phi_\nu(\boldsymbol{x}) \tag{2}$$

and the spontaneous emission is described by

$$\sigma_\nu(\boldsymbol{x}) = \frac{h\nu}{4\pi} n_2(\boldsymbol{x}) A_{21} \Phi_\nu(\boldsymbol{x}), \tag{3}$$

where $\Phi_\nu$ denotes the Doppler profile. For a two-level system the equations of statistical equilibrium are

$$\begin{aligned} \frac{dn_2}{dt} &= B_{12} n_1 J_\nu - B_{21} n_2 J_\nu + p_2 - \Gamma n_2 - A_{21} n_2, \\ \frac{dn_1}{dt} &= B_{21} n_2 J_\nu - B_{12} n_1 J_\nu + p_1 - \Gamma n_1 + A_{21} n_2, \end{aligned} \tag{4}$$

with

$$J_\nu = \frac{1}{4\pi} \int I_\nu(\Omega)\, d\Omega. \tag{5}$$

Here the $p_i$ denote the pump rate into level $i$ (the upper level is 2) from levels other than the maser levels (the reservoir) and $-\Gamma n_i$ denotes the loss to the reservoir from level $i$ with $\Gamma$, the inverse lifetime of the maser states, taken the same for both levels. $A_{ij}$ and $B_{ij}$ denote the Einstein coefficients for spontaneous and induced emission, respectively.

Note that the induced emission term in the equations of statistical equilibrium is expressed as the integral of the intensity over $4\pi$ sr. In this way the transfer problem has become more dimensional. Indeed, due to the extent of the circumstellar shells around OH/IR stars, beams of radiation propagating in different directions may cross and compete for the same inverted molecules. In all the cases we consider, two-dimensional radiative transfer will suffice. Three-dimensional solutions are only needed in sources that are truly three-dimensional in nature. In other cases (even in a purely spherical problem) we have to treat the problem in at least two-dimensions, because radiation in radial and tangential directions behaves differently. In the rest of the paper we will only consider two dimensions, although the extension to three dimensions is trivial, but computationally costly.

When we examine the above equation somewhat closer, two properties are immediately evident. The first is that the physics is described by local equations but, in order to solve the radiative transfer problem, we need a global solution of these equations. This is a very general statement applicable to any transfer problem. In some cases a local approximation may be found, such as in the Sobolev or escape probability approximation. But, since OH/IR stars are devoid of any large velocity gradients, these concepts cannot be used: the $J_\nu$ term may pick up contributions from the whole medium, so the specific intensity $I_\nu$ cannot be determined locally. The second property is the non-linear and coupled nature of the equations. Solving the radiative transfer equation means that we have to solve the equations of statistical equilibrium for the level populations or, equivalently, the optical depth. But these level populations depend on the integral of the radiation field we want to determine. So the problem as formulated above is coupled in a non-linear way.

### 2.2 Saturation and beaming

Since we are dealing with a maser medium ($\alpha_\nu < 0$), a beam of radiation travelling in a particular direction will be amplified exponentially. On the other hand, the inversion in the medium is maintained by the pump process. Now as long as the intensity is small, the inversion in the medium will hardly be affected by the growing intensity. This is equivalent to saying that the $J_\nu$-term in the equations of statistical equilibrium is small. In this regime the transfer problem is essentially one-dimensional, since the level populations may be determined independently and the intensity in a particular direction is a simple line integral over this distribution. This, by the way, does not imply that the maser is not beamed. Because some paths through the medium are longer and the amplification is exponential, the radiation preferentially flows along the longest path.

When the intensity is large it will deplete the ambient inversion. Since the pump rate is an upper bound to the number of maser photons which may be created per unit time, an equilibrium will result between the radiation field

and the level populations; the maser saturates and the pump photons which lead to inverted molecules are directly converted into maser photons. Elitzur (1982) aptly calls a saturated maser a 'linear converter', in the sense that the resulting luminosity is proportional to the total (volume-integrated) pump rate. This means that the non-linear coupling between equations (1) and (4) through the $J_\nu$-term will not be small.

The fact that the maser turns into a linear converter does not imply that the solution for $I_\nu$ is obtained easily. On the contrary, different directions become coupled through the strong interaction between the level populations and the radiation field. Suppose that a strong and a weak beam of radiation cross at some place in the medium. The strong one possesses more maser photons and will therefore be able to induce more stimulated emission leading to higher gain. Thus there will be fewer inverted molecules left for the weak beam. So the strong beams propagating through the medium may quench the growth of the weak ones by 'eating away' the available inverted molecules.

As long as this happens in the unsaturated regime, the transfer problem is essentially one-dimensional and the effect of beam crossing is minimal. But in the saturated regime we need to distribute the inverted molecules over the appropriate directions. Since the strong beams will de-excite the majority of these molecules, the radiation field will develop an *additional* anisotropy. That is, the concept of linear conversion is still true but the distribution of additional maser photons over different directions depends on the angular properties of the radiation field.

For the case of a spherical shell the geometry alone would, even for an unsaturated maser, produce anisotropic radiation. Since maser amplification requires velocity coherence, an expanding shell will make things even more complicated. And finally, when the maser is saturated, the two-dimensional effect of beam crossing enhances this anisotropy even further. The effect of beam crossing has been discussed by several authors. Elitzur (1990a) and Alcock & Ross (1985a, b) give a clear description of the differences between one- and two-dimensional transfer and the essential role played by saturation.

It is obvious that, since the problem is non-linear, non-local and two-dimensional, an analytic solution will be hard to obtain in general. We therefore solve the radiative transfer problem numerically using a Monte Carlo method.

## 3 A MONTE CARLO APPROACH

### 3.1 Flow of the code

The technique of solving radiative transfer problems with Monte Carlo schemes is not new (e.g. Bernes 1979). The basic idea is that we use a limited number of 'photon packages' to represent the radiation field. In this way we find a global solution in the same way that nature does: the individual photon packages produce a global solution of the complicated two-dimensional radiative transfer problem, by travelling through and interacting with the medium. This method can thereby simulate the radiative transfer of the complex form we see in a maser.

The Monte Carlo method is limited by statistics, in that a limited number of packages results in a noisy model. But we also have to demand that the resolution in, for instance, time and space, is sufficient to follow the physics. Nature (again) uses a large number of packages to establish this: a circumstellar 1612-MHz maser produces $\approx 10^{43}$ photons per second.

We will start with a medium in which we keep track of the physical conditions: we divide our medium up in to cells which have a density, population distribution, pump rate and a velocity. The size of these cells should be such that we can resolve the changes of the physical conditions with position in the medium. As a rule of thumb we suppose that the cells should be of size $< l_{\rm mfp}$ (the photon mean free path). In order to make the code more efficient one can also use symmetry considerations to cut down the number of cells. For instance, in a spherical case the physical conditions of the medium are only a function of radius, although a two-dimensional solution for the radiation field is necessary. In the present case, we have chosen to use a full grid for practical considerations.

Through this grid we send a large number of photon packages with which we simulate the radiation field. The photons in each package are all in the same radiation mode. There is a characteristic time-scale for these photon packages to interact with the medium, which is $t_{\rm int} = l_{\rm mfp}/c$. Thus we calculate the new position of all the photon packages after they have travelled $\hat{l}_{\rm mfp}$, an *a priori* estimate of the mean free path in the medium (we will later use $l_{\rm mfp} \approx 10^{14}$ cm); then they interact with the level populations of the grid cell they are in. We do this for all packages until they leave the grid and can be observed. Again we must ensure that enough packages are taken into account to describe the physics accurately. Typically there should be about as many photon packages as there are cells in the grid ( $\sim 30\,000$). If this condition is not satisfied, the time-scale for the depletion of the inversion is not adequate to match the pump rate. Then a cell might go through different pump cycles before being hit by a photon package.

Notice that the choice of the step size $\hat{l}_{\rm mfp}$ does not predetermine the resultant solution. Although $\hat{l}_{\rm mfp}$ may differ from the true local $l_{\rm mfp}$ at a given time, as long as it does not exceed $l_{\rm mfp}$ it will only slow down our calculations. For every step, we calculate in every cell the local absorption coefficient, $\alpha$, which is determined from the local level populations and contains all the interesting interactions between the radiation field and the medium. We calculate the corresponding $l_{\rm mfp}$ which should be larger than $\hat{l}_{\rm mfp}$. After each step of $\hat{l}_{\rm mfp}$ the number of photons in each package is modified according to

$$n'_{\rm php} = n_{\rm php} \exp[-\alpha_\nu(\boldsymbol{x})\,\hat{l}_{\rm mfp}]. \qquad (6)$$

The inversion is then reduced by the same number. The total number of inversions is, of course, an upper limit to the growth of the photon package (saturation!).

There is an important fact that makes this process feasible for a maser medium. Due to exponential amplification, the $J_\nu$-term in equation (4) will start to dominate over spontaneous emission very rapidly, so that spontaneous emission is only important to start up the maser but does not influence the level populations significantly. Because the total radiation mode for stimulated emission is conserved, we only have to change the number of photons in each package (we will call this the 'multiplicity' of a package). We can keep track of the

stimulated emission without changing the total number of photon packages in the computer. This fact makes the Monte Carlo approach very well suited for maser emission.

After we have taken a time-step in this way, we update our level populations. In each cell there can be a specific pump; we now integrate the pump rate over $t_{\rm int}$ and calculate the new level populations. This is also the time to create randomly new photon packages due to spontaneous emission (we neglect other input sources such as a background star for the moment). Notice that the creation of random photon packages is the Monte Carlo part of the approach. We use a random number generator to pick the place, direction and thermal velocity component of the new photon packages. The initial multiplicity of a package is then determined by the local level populations of the cell where it was created. In principle it is straightforward to add also contributions from background sources here.

When a photon package leaves the grid we record its multiplicity, direction, frequency, and the position where it emerges, in order to calculate observables such as spectra.

### 3.2 Accuracy

It is important to realize that the global solution will not (in a mathematical sense) converge. The code gives a representation of a 'physical' situation at any time. The time-scale for the model to reach an equilibrium is $\approx t_{\rm cross} = l_{\rm max}/c$, the crossing time for a photon, because this is the time-scale on which all parts of the medium communicate with each other. Here $l_{\rm max}$ is the longest path in the medium. After such a time the model will fluctuate around a stable state, the deviations being caused by statistical fluctuations.

If we continue to run the model for $t > t_{\rm cross}$, we do not reach a better solution, but we do obtain more solutions. That is, we find more realizations of the same physical equilibrium at different times, but each may be slightly displaced from the mean due to the $\sqrt{N}$ Monte Carlo statistics. We can average these different realizations to improve our statistics.

These considerations also limit the resolution of our code. If, for instance, we want to compute the spatial intensity distribution (or equivalently brightness temperatures) from some part of the medium, we will have to divide our photon packages over a great number of bins in position and direction. The $\sqrt{N}$ statistics will then put a severe constraint on the possible resolution.

## 4 RESULTS FOR A RECTANGULAR GRID

To test whether the adopted approach works, simulations were done for a maser in a rectangular medium. In particular we used a four-stream model in a homogeneously pumped static medium. This radiation field consisted of beams that could travel in only four directions: east, west, north and south. We did not need to sample the intensity for this problem with a higher resolution in direction, since a four-stream model contains all the two-dimensional physics necessary to investigate the effects of beam crossing. Apart from that we were able to compare our results easily with a code in which the beam crossing was switched off. Figs 3 and 4 show the results of these investigations. First there is the unsaturated core in Fig. 3, which clearly shows the transition from an unsaturated to a saturated domain for a partially saturated model. It is in the saturated region that one expects the two-dimensional effect of beam crossing to be most effective. It is worth mentioning that the unsaturated core in a maser was predicted in the work of Elitzur (1990b), who derived this result using general arguments.

To investigate the effect of beam crossing in a qualitative way we have calculated a number of models with different axis ratios. Figs 4(a) and (b) show the results of these calculations. The curves show the intensity ratio as a function of axis

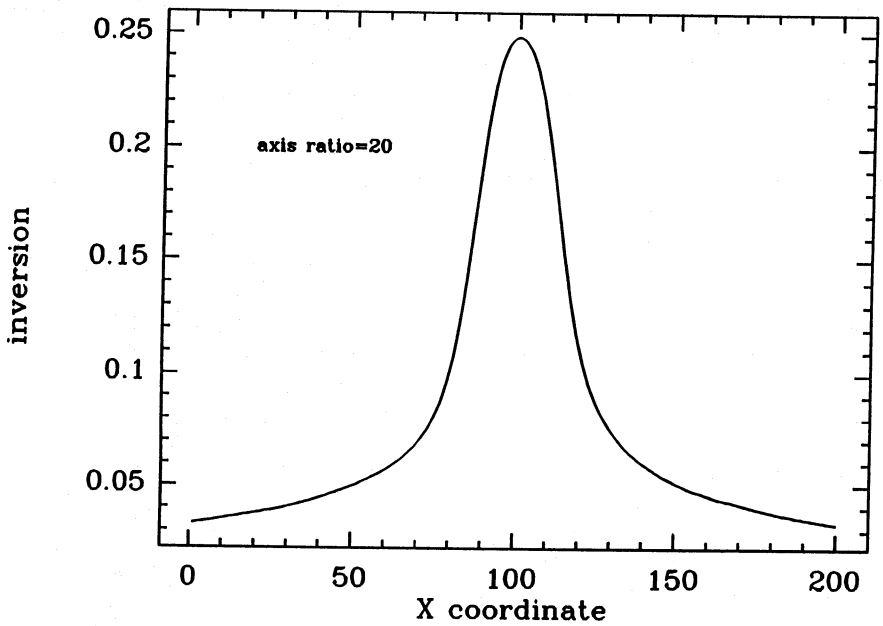


**Figure 3.** A cross-cut of the grid along the long axis. The relative inversion is shown, the unsaturated core is clearly visible.

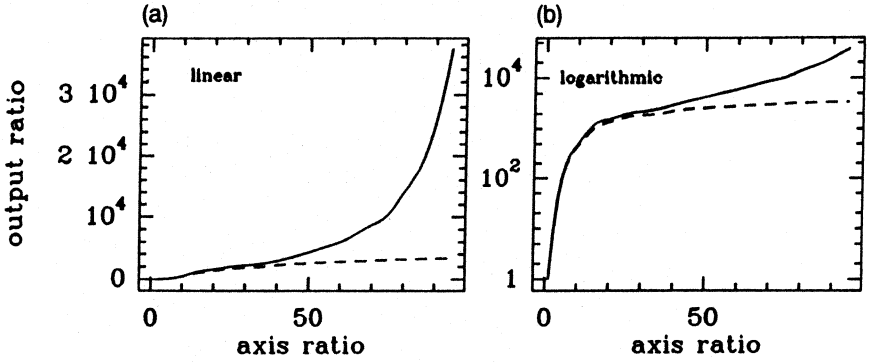


**Figure 4.** (a) The ratio of flux that emerges from the long axis of a grid to that of the short axis as a function of axis ratio. (b) As (a), but now the ratio of emergent flux is shown on a log scale.

ratio, where we have divided the east–west beam along the long axis by the north–south beam along the short axis. For larger axis ratios (we keep the short axis fixed), more and more path-length in the east–west direction is available. Thus those models are more strongly saturated. The upper curve represents the solution of the complete two-dimensional radiative transfer problem. The lower curve, on the other hand, is the one-dimensional result in which the four streams are artificially decoupled, so that the effect of beam crossing has not been taken into account. The difference between the curves is evident: as long as the maser models are saturated, the inversion is little affected by the propagating beams and the problem is effectively one-dimensional. But as we move towards saturated models, the stronger (dominant) beams will quench the growth of the weaker ones more and more effectively, creating an even more anisotropic radiation distribution. Notice that, because the axis ratio is much larger than unity, the unsaturated core will extend all the way through the north–south direction, dissecting the maser. This has been verified numerically. So there will always be beams which have travelled through the unsaturated core, making them dominant over the others.

These results clearly show that the effect of beam crossing, at least qualitatively, is present. In a series of papers Alcock & Ross (1985a, b) investigated the effect of beam crossing also using a four-stream model. Instead of adopting a Monte Carlo method, they derived a set of four coupled differential equations which they integrated numerically. Their four-stream model shows the same behaviour qualitatively, which is encouraging, because the two approaches to the problem are quite different.

## 5 MODELLING CIRCUMSTELLAR SHELLS

### 5.1 Spherical grids

To model circumstellar shells we define the cells in the appropriate geometry, namely polar coordinates. Because the shell is expanding, each cell has a velocity with respect to an observer. Since the velocity field is radial this is very easy to code in polar coordinates. On top of this systematic velocity we also add a distribution of thermal velocities, due to the non-zero temperature of the emitting gas. With the random number generator, this thermal velocity component for each emitted photon is chosen, accordingly to a Gaussian Doppler profile.

The problem is still spherically symmetric (but not isotropic), so that an observer at any location around the OH/IR star should see the same spectrum (and spatial intensity distribution). Let us consider the observable spectrum. To make optimal use of all the photon packages, we may add all the spectra and average them over all possible observers. That is, there is an observer for each direction into which we have randomly sent photon packages due to spontaneous emission. Adding up all the spectra, we use photons that travel in any direction. Thus we can calculate a flux $F_\nu$ for comparison with observations. This was coded in a program called cOHERENCE in order to investigate the properties of circumstellar OH masers.

### 5.2 Input parameters

The input parameters for cOHERENCE and the conditions of the medium are listed below for what we will call the standard model.

The expansion velocity is taken to be 20 km $s^{-1}$ and is assumed to be constant throughout the shell. This value (or the ratio of expansion velocity and Doppler width) is just an arbitrary scaling parameter. Several studies have tried to investigate the acceleration of the outflow with radius, but it is almost impossible to measure this within the OH region. From a theoretical point of view, the assumption of constant velocity seems justified (Goldreich & Scoville 1976). Because the formation of OH, in the region where the maser operates, is so far from the central star, the acceleration of the shell by radiation pressure will be negligible there.

The Doppler profile of the OH molecules is represented by a Gaussian profile with a FWHM of 1.0 km $s^{-1}$. This width is somewhat larger than expected from the temperature of the gas at $3 \times 10^{16}$ cm (Goldreich & Scoville 1976), but this is chosen to mimic the possible turbulence in the shell (e.g. Diamond *et al.* 1985).

The simple model presented here uses a constant pump rate. A constant fraction of the OH molecules is transferred to a higher energy level at every time-step. This ignores radial dependence of the IR radiation field, the local optical depth in the pump line and line overlap. These features could be coded into cOHERENCE with relative ease. The constant

pump rate is estimated from the average physical conditions in the shell, following the cycle as described by Elitzur, Goldreich & Scoville (1976). Here the maser is pumped by far-infrared (FIR) dust emission at a wavelength of 35 $\mu$m. The dust temperature is assumed to be ~150 K and the spectrum of the dust emission then follows a diluted blackbody. The amount of 35-$\mu$m absorption in a cell is estimated from the average OH density. The necessary Einstein $A$ coefficients for this and for the spontaneous decays are taken from Destombes *et al.* (1977).

The OH density is taken to be constant at $n_0 = 2$ cm$^{-3}$ between an outer and inner radius (Goldreich & Scoville 1976; Netzer & Knapp 1987).

The region where the maser operates lies between $2.5 \times 10^{16}$ and $3.5 \times 10^{16}$ cm. We have quite good measurements of the radius of the maser from phase lags (Herman & Habing 1985; van Langevelde *et al.* 1990). These show that the diameters of the shells are typically 30 light-days ($6 \times 10^{16}$ cm). The thickness of the shell is more difficult to obtain, and *cannot* be estimated from a map of the shell. Because the maser is beamed (saturated or not) the thickness of the shell will always appear smaller. Theoretical work by Netzer & Knapp (1987) indicates thick shells. In our model we use a shell which could be considered thick.

### 5.3 Results

Now we consider the results of our models for OH/IR stars. Fig. 5 shows a spectrum calculated with the values of the standard model. The total simulation modelled six crossing times; the spectrum shown is the average over the last four of these. We have derived other observables as well which are not displayed here. We used a grid with a spacing of $1 \times 10^{14}$ cm. The total number of photon packages was $\approx 8 \times 10^6$. The result was obtained on the CONVEX C220 of the Leiden University in 30 CPU hours. The spectrum shows a striking resemblance to observed profiles. The fluctuations in the simulated spectrum are a result of the $\sqrt{N}$ statistics of the Monte Carlo approach and will decrease if the number of photon packages is increased.

As Fig. 1 shows, the spectra of real OH/IR stars also exhibit irregularities, but since all our models are homogeneous we are not capable of reproducing them. However, it should be realized that a small amount of inhomogeneity suffices to account for this. For a saturated maser the intensity is a strongly beamed portion of $J_\nu$,

$$I_\nu = \frac{4\pi}{\Delta\Omega} J_\nu. \tag{7}$$

Following Elitzur (1990a) we argue that, roughly speaking, $\Delta\Omega \approx \tau^{-2}$ and $J_\nu \approx \tau$, so that relative changes in optical depth (either due to velocity turbulence, density irregularities or non-uniform pumping) will be enhanced by a factor of 3 in the intensity. In this view, an irregular feature on an OH spectrum should not necessarily be interpreted as coming from a more luminous region of the shell, because an observer in a different direction might observe this same region as a dip in the spectrum.

The flux scale of the spectrum was calculated assuming a distance to the object of 1 kpc, which is a reasonable distance for an average OH/IR star. Nevertheless, we have some practical problems reproducing objects at the high end of the luminosity function (such as shown in Fig. 1); in order to model these objects we have to increase the pump rate and/or OH density. This implies a smaller $\hat{l}_{\rm mfp}$ and thus more grid cells. As the computing time scales as $\hat{l}_{\rm mfp}^{-3}$, this is not feasible at present.

We emphasize here that the spectral shape produced by our method is not a strong function of input parameters.

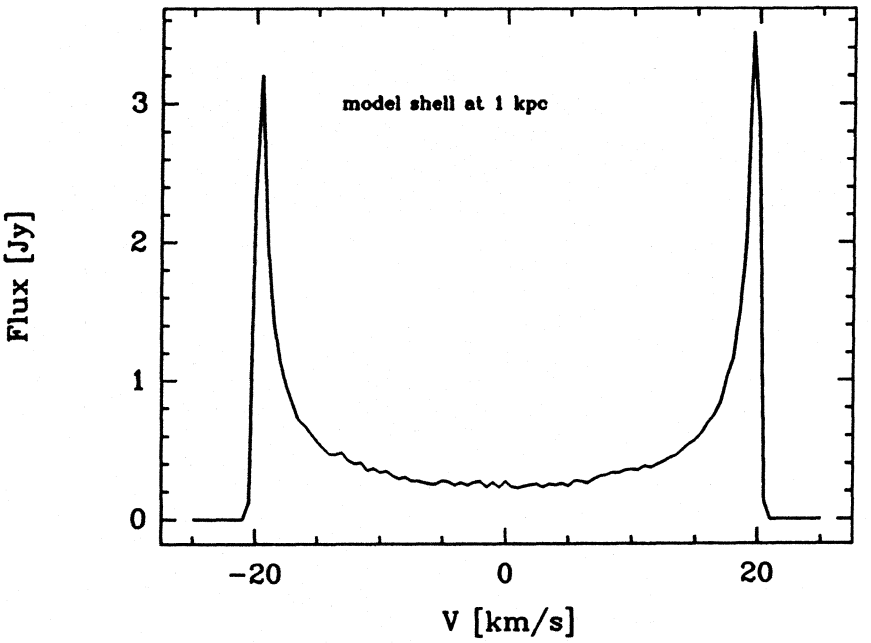


**Figure 5.** The simulated spectrum of our 'standard model'.

Physical parameters such as thickness, pump rate and density, as well as the internal parameters that govern the resolution of the code, such as $\hat{l}_{\rm mfp}$, can all be varied within reasonable values and still COHERENCE produces an OH/IR star.

Work on the modelling of the observational properties of OH/IR stars has also been done by Alcock & Ross (1986a, b), where they extend their four-stream model to the case of circumstellar shells. They have great difficulties in constructing spectra which resembles the observations and, in order to get acceptable spectra, they have to fine-tune their parameters extensively. This leads them to reject the standard model and to propose an alternative structure of the shells by introducing inhomogeneities (which they call platelets) in the shell. We are able to construct convincing models for a large set of parameters using just the standard model. We do not know the cause of the discrepancy between their results and ours. The two approaches are fundamentally different and it is therefore difficult to compare them in a straightforward manner.

## 6 CONCLUSIONS

We have shown that a Monte Carlo simulation offers a very transparent way to model the complicated radiative transfer in masers. It is capable of reproducing important effects such as saturation and beam crossing. A big advantage is that everything is coded in local physics. This, in principle, makes it straightforward to simulate complicated situations such as velocity fields, detailed pump mechanisms and density fluctuations. A disadvantage is that more detail requires more random photon packages. This will make it, for instance, very expensive to study the anisotropies introduced by inhomogeneity.

When we use the code to simulate an OH/IR star in a circumstellar shell, we find that a rough estimate of the parameters reproduces a spectrum which closely resembles the average spectra of OH/IR stars. We thus argue that extra assumptions which have been proposed before are superfluous. In particular, we do not need the 'platelets' proposed by Alcock & Ross (1986a). We are convinced that small density and/or velocity irregularities can account for the deviations from the smooth spectrum in true astrophysical masers.

## ACKNOWLEDGMENTS

We thank Harm Habing, Vincent Icke and Ewine van Dishoeck for their encouraging interest in our work.

## REFERENCES

Alcock, C. & Ross, R. R., 1985a. *Astrophys. J.*, **290,** 433.
Alcock, C. & Ross, R. R., 1985b. *Astrophys. J.*, **299,** 763.
Alcock, C. & Ross, R. R., 1986a. *Astrophys. J.*, **305,** 837.
Alcock, C. & Ross, R. R., 1986b. *Astrophys. J.*, **306,** 649.
Bernes, C., 1979. *Astr. Astrophys.*, **73,** 67.
Booth, R. S., Kus, A. J., Norris, R. P. & Porter, N. D., 1981. *Nature,* **290,** 382.
Bowers, P. F. & Johnson, K. J., 1990. *Astrophys. J.*, **354,** 676.
Bowers, P. F., Johnson, K. J. & Spencer, J. H., 1983. *Astrophys. J.*, **274,** 733.
Cohen, R. J., 1989. *Repts Prog. Phys.*, **52,** 881.
Destombes, J. L., Marliere, C., Baudry, A. & Brillet, J., 1977. *Astr. Astrophys.*, **60,** 55.
Diamond, P. J., Norris, R. P., Rowland, P. R., Booth, R. S. & Nyman, L.-Å., 1985. *Mon. Not. R. astr. Soc.*, **212,** 1.
Elitzur, M., 1982. *Rev. Mod. Phys.*, **54,** 1225.
Elitzur, M., 1990a. *Astrophys. J.*, **363,** 628.
Elitzur, M., 1990b. *Astrophys. J.*, **363,** 638.
Elitzur, M., Goldreich, P. & Scoville, N., 1976. *Astrophys. J.*, **205,** 384.
Goldreich, P. & Scoville, N., 1976. *Astrophys. J.*, **205,** 144.
Herman, J. & Habing, H. J., 1985. *Astr. Astrophys. Suppl.*, **59,** 523.
Herman, J., Baud, B., Habing, H. J. & Winnberg, A., 1985. *Astr. Astrophys.*, **143,** 122.
Jewell, P. R., Webber, J. C. & Snyder, L. E., 1980. *Astrophys. J. Lett.*, **242,** L29.
Johansson, L. E. B., Andersson, C., Goss, W. M. & Winnberg, A., 1977. *Astr. Astrophys.*, **54,** 323.
Lindqvist, M., Winnberg, A. & Habing, H. J., 1989. In: *From Miras to planetary nebulae: which path for stellar evolution?* p. 259, eds Mennessier, M. O. V. & Omont, A., Editions Frontières, Gif sur Yvette.
Lindqvist, M., Winnberg, A., Habing, H. J. & Matthews, H. E., 1992. *Astr. Astrophys. Suppl.*, **43,** 43.
Netzer, N. & Knapp, G. R., 1987. *Astrophys. J.*, **323,** 734.
Schultz, G. V., Sherwood, W. A. & Winnberg, A., 1978. *Astr. Astrophys. Lett.*, **63,** L5.
van Langevelde, H. J., van der Heiden, R. & van Schooneveld, C., 1990. *Astr. Astrophys.*, **239,** 193.
Wilson, W. J. & Barrett, A. H., 1968. *Science,* **161,** 778.